Submitted to Industrial & Engineering Chemistry Research

https://doi.org/10.1021/acs.iecr.9b05548

Direct non–oxidative methane coupling to ethylene over gallium nitride. A catalyst regeneration study.

Kanchan Dutta, Mohsen Shahryari, Jan Kopyscinski*

Department of Chemical Engineering, McGill University,

3610 University Street, Montreal, Quebec H3A 0C5, Canada

* To whom all correspondence should be addressed:

Tel.: +1 514 398 4276

jan.kopyscinski@mcgill.ca

Abstract

The abundance of methane in natural and shale gases creates the need to develop processes for the direct conversion of methane to olefins, aromatics, and hydrogen. In this work, the regeneration capability and reusability of gallium nitride (GaN) catalysts for the direct non-oxidative methane activation with subsequent coupling to ethylene were studied. Unsupported GaN as well as silica-supported GaN/SBA15 catalysts were synthesized and evaluated. Each catalyst was subjected to two different regeneration methods. In the first method, the used catalysts were regenerated with air at 500-550 °C and reused several times. Due to the slight oxidation of the surface GaN to Ga_2O_3, the ethylene yield decreased by 16% after 5 cycles. The second method included an intermediate re-nitridation step after air regeneration to convert the surface Ga_2O_3 back to GaN. By doing so, the ethylene yield remained constant over multiple cycles.

1 Introduction

Methane is readily found in nature in the form of natural and shale gases. According to the U.S. Energy Information Administration's International Energy Statistics, the total proved reserves of gross natural gas is 200 trillion m^3 (2018). Methane is currently used to produce synthesis gas, which is of a mixture of carbon monoxide and hydrogen. This syngas can then be converted to methanol, or directly to hydrocarbons through the Fisher-Tropsch process[1]. Not only is this process energy and capital intensive[2], but it also produces carbon dioxide, a greenhouse gas.

Direct non–oxidative conversion of methane to olefins and aromatic compounds is a favorable alternative to the aforementioned process as it provides an efficient and environmentally friendly method for converting methane. Most catalysts used for direct non–oxidative methane conversion are currently based on Mo-Zeolite systems to produce benzene predominately with only little olefins[3–5]. Coking and hence, catalyst deactivation is still the main obstacle. Generally, two approaches exist to improve methane conversion and product selectivity, and to deal with the coking: (1) catalyst development and (2) reaction engineering. Catalyst performance has been improved by support optimization for suppressing coking[3,4]. Dealumination of the zeolite support or silanation methods were used to reduce the number of acid sites that facilitate coking. Adding promoters was another way; transition metals in Period 4 (Fe, Co, Ni, Cr, Cu, Zn) and metals in Group 13 (Ga and Al) show improvement in terms of methane conversion and catalyst stability[6–8].

In another approach, the inhibition of coking was achieved by preparing an iron silica catalyst with an isolated monoatomic iron site embedded in a silica matrix[9]. It was hypothesized that the absence of an adjacent iron site hinders catalytic C–C coupling and thus catalyst deactivation. However, reaction temperature of more than 1000 °C was required that produced ethylene (40-48%), naphthalene (20-30%), and benzene (25-30%).

Commercial GaN material was shown to be highly active towards methane aromatization under photocatalytic conditions at room temperature, and thermocatalytic conditions up to 450 °C in a batch reactor with residence times of 5-8 h[10,11]. In both cases, benzene selectivity of up to 90% was achieved without any significant coking. Based on these results, we developed unsupported and supported GaN (on mesoporous high surface area silica, SBA-15) catalysts, and studied methane activation at higher temperatures (700 °C) and 1 bar pressure in a flow reactor with short residence times (1-3 s)[12]. Under these conditions, methane conversion of 0.5% was achieved, and ethylene (selectivity > 95%) was the main hydrocarbon product instead of benzene. However, carbon deposition was inevitable (10 to 22 $mg_C\ g_{cat}^{-1}$). PtSn-zeolite catalysts were developed for the non-oxidative methane coupling to ethylene[13]. At 700 °C, they achieved methane conversions of max 0.3% and ethylene selectivities of 70-90% (hydrocarbons only) with a much higher carbon deposition of 43 to 120 $mg_C\ g_{cat}^{-1}$. The addition of Sn helped to redisperse Pt nanoparticles, especially during the oxidative regeneration process[14]. Equilibrium conversion from methane to ethylene at 700 °C is ~4%.

From the process design standpoint, the addition of co-reactants, coupling methane activation with other reactions (e.g., methane reforming, oxidative coupling), changing residence time, and the introduction of regeneration cycles have been explored to reduce coking or remove coke deposition to extend the catalyst lifetime[5,15]. Coking is unavoidable, which makes catalyst regeneration a crucial step. Besides fixed bed reactors, various fluidized bed reactors with and without regeneration cycles have been applied. It is common to regenerate the catalysts with air at high temperature to burn off the carbon deposition[3,16]. Hydrogen at 900 °C has also been used for the regeneration process[17].

In this work, we present an experimental study on various regeneration procedures for unsupported and supported GaN/ SBA15 catalysts. Additionally, we report an effective protocol consisting of activation/ regeneration/re-nitridation cycles that extend the catalyst life. The re-nitridation step allows restoring the active surface gallium–nitride after each regeneration step in air in which surface gallium-oxides are formed.

2 Experimental Section

2.1 Catalyst preparation

Both unsupported gallium nitride (GaN) and supported GaN/SBA15 catalysts were synthesized following the procedure developed and described in our previous work[12,18].

Unsupported catalysts were synthesized using evaporation induced self-assembly (EISA) method[19]. Around 1 g of a triblock copolymer (Pluronic P-123, Sigma Aldrich) was dissolved in 15 mL of pure anhydrous ethanol (C_2H_5OH, Greenfield Global Inc.) by stirring the mixture for 30 min at 600 rpm. Around 1.5 mL of nitric acid (HNO_3, 67-70 wt%, Fisher Scientific) was then mixed with the copolymer solution. After 15 min, a $Ga(NO_3)_3 \cdot xH_2O$ solution (4 g of nitrate salt in 5 mL DI water and 5 mL of ethanol) was added, and the mixture was left under constant stirring for 5 h. The solution was dried at 60 °C for 48 h, and the solid was subsequently calcined at 650 °C for 6 h (1 °C min^{-1}) to form Ga_2O_3 powder.

SBA-15 synthesis was based on the method described in[20]. In a typical synthesis, 4 g of P-123 copolymer was dissolved in 95 mL of DI water and 4 mL of hydrochloric acid (36-38% HCl, Fisher Chemical). The solution was stirred at room temperature at 600 rpm for several hours to ensure complete dissolution of the copolymer. The clear solution was heated to and held at 38.5 °C. Then, 9.5 mL of tetraethoxysilane (TEOS, 99.9%, Alfa Aesar) was added under stirring (600 rpm). The solution was left under stirring (600-700 rpm) for 24 h at 38.5 °C. The opaque white solution was subjected to hydrothermal treatment inside closed polypropylene DigiTUBEs (SCP science) at 100 °C for 48 h and then filtered under vacuum to collect the precipitate. The precipitate was washed several times using DI water (150-200 mL total using

10 mL increments). The residue on the filter paper was dried overnight at 60 °C, transferred to ceramic boats, and then calcined at 550 °C for 6 h (1 °C min^{-1}) to obtain SBA-15. Incipient impregnation was employed to prepare the supported catalysts. Dry gallium (III) nitrate hydrate powder ($Ga(NO_3)_3 \cdot xH_2O$, 99.9998 wt% trace metal basis, ACROS Organic, Thermo Fisher Scientific) was used as the Ga precursor. The amount of precursor required to obtain the target loading of 16 wt% Ga stoichiometrically was weighed. As gallium (III) nitrate is hygroscopic, the powder was always stored under dry argon (Ar, 99.999%, with < 5 ppm moisture, Praxair) in a desiccator to prevent moisture absorption. The bottle was also flushed with Ar after every use. The aqueous nitrate solution (in DI water) was used for the incipient impregnation. Approximately 4.5 mL of solution was used for 1 g of SBA-15. After impregnation, the incipiently wet solid was left overnight at room temperature and subsequently dried at 60 °C for 8 h. Finally, the dried solid was calcined at 550 °C for 6 h (1 °C min^{-1}) and labeled Ga_2O_3/SBA15.

Both powders (Ga_2O_3 and Ga_2O_3/SBA15) were nitridated with anhydrous ammonia (NH_3, 99.99%, Megs Specialty Gases, 20 mL$_S$ min^{-1}) at 750 and 700 °C, respectively, in a fixed bed reactor, as described in our previous work (subscript S denotes standard condition with $T = 0$ °C and $p = 1.013$ bar$_{abs}$). Before nitridation, the Ga_2O_3 or Ga_2O_3/SBA15 powder was dried at 300 °C for 4 h under Ar (15-20 mL$_S$ min^{-1}) followed by a gradual temperature increase to 750 or 700 °C (1.5 °C min^{-1}) under NH_3 atmosphere. The samples were nitridated for 6.5 h at the nitridation temperature and then cooled to room temperature under continuous NH_3 flow. The catalyst remained in contact with ammonia for a total period of 24 h. The nitride catalyst was then stored in a vial filled with Ar and placed in an Ar purged desiccator cabinet. The unsupported and supported samples were named GaN and GaN/SBA15, respectively. The catalysts had a particle size between 150-600 µm. The GaN catalysts were dark yellowish-brown in color, while the GaN/SBA15 samples were bright yellow (Figure S1).

2.2 Catalyst characterization

Physical characterization of the synthesized catalysts was carried out using nitrogen adsorption/desorption measurements (–196 °C). The properties analyzed were total surface area, pore size distribution, and pore volume. Measurements were conducted using a Micromeritics Tristar 3000 BET analyzer. Before the analysis, the samples were degassed under vacuum for 12 h at 250 °C.

X-ray diffraction was used to identify the crystalline phases in the materials synthesized. Analyses were conducted on a Bruker D8 Discovery X-Ray Diffractometer with a two-dimensional VANTEC-500 detector and a CuK_α (λ = 1.5406 Å) radiation source. The tube voltage was 40 kV, the tube current was 20 mA, and the scan rate was 5° min^{-1}.

Ga content of the supported catalyst GaN/SBA15 was determined by Inductively Coupled Plasma - Optical Emission Spectroscopy (ICP-OES, iCAP 6500 dual view Thermo Scientific). The catalyst was fused with twice the amount (by weight) of lithium tetraborate (SCP science) in a 9 mL graphite crucible (SCP science). The fusion was performed in a muffle furnace while gradually increasing the temperature to 950 °C, where it was subsequently held constant for 30 min. A glassy bead was obtained after cooling. The fusion flux was carried out in triplicates. Two different solutions were prepared from the bead; one in a 10% HNO_3 (trace metal grade) and the other in a 3:1 HCl to HNO_3 concentrated solution (aqua regia). Dissolution was carried out in polypropylene DigiTUBEs at 95 °C for 2 h until the bead was completely dissolved and a clear transparent solution was achieved. Once cooled, the solutions were filtered through a 45 µ filter and diluted appropriately for ICP analysis. Unsupported catalysts were made exclusively of Ga_2O_3, GaN, or of a mix of both; no other metals were present. Gallium content in unsupported catalysts can also be calculated directly without ICP.

The total nitrogen content of unsupported gallium nitride catalysts was determined using a Shimadzu TOC-Vcph with a TNM-1 Total Nitrogen Module. Before the analysis, 25-50 mg of the catalyst sample was dissolved in 6M HCl at 80 °C. The gallium nitride was converted to gallium chloride and ammonium chloride (eq. 1), while gallium oxide was dissolved in the acid to produce gallium chloride (eq. 2).

$$\mathrm{GaN}\ (s) + 4\ \mathrm{HCl}\ (aq.) \rightarrow \mathrm{GaCl_3}(aq.) + \mathrm{NH_4Cl}\ (aq.) \tag{1}$$

$$\mathrm{Ga_2O_3}\ (s) + 6\ \mathrm{HCl}\ (aq.) \rightarrow 2\ \mathrm{GaCl_3}\ (aq.) + 3\ \mathrm{H_2O} \tag{2}$$

The clear homogenous solution was cooled and then diluted with deionized water to obtain a pH between 2 and 3. The diluted solution was analyzed to determine the total nitrogen content. Before each analysis, the instrument was calibrated using several ammonium standards (Sigma Aldrich) containing 1000 mg L^{-1} of N in the form of NH_4^+ in water. The pH of the calibration solutions was adjusted to be between 2 and 3 by using HCl. However, this method did not work for the supported catalysts as HCl was incapable of extracting GaN from the support, proven by ICP analysis of the corresponding solution.

Scanning Electron Microscopy (SEM) analysis was performed using a FEI Inspect F-50 field emission scanning electron microscope on the fresh, spent, and regenerated unsupported GaN. Also, Energy-Dispersive X-ray Spectroscopy (EDS) experiments were performed for elemental analysis (Ga, N, O, and C) of the samples.

Temperature programmed oxidation - mass spectrometry (TPO-MS) analysis was performed on the fresh and spent catalysts to quantify the amount of deposited coke (and inherent carbon, if any, in the fresh catalyst). In the analysis, 50 mg of supported and 100 mg of unsupported catalyst was loaded in a quartz tube and inserted in a stainless-steel reactor (the same reactor used for regeneration, see below). The sample was dried at 110 °C for 2 h and then heated from room temperature to 950 °C with a ramp rate of 5 °C min^{-1} under air (Ultra Zero Air, MEGS Specialty Gases, 22 mL_S min^{-1}). The product gas at the reactor outlet was electrically heated to 200 °C, mixed with Ar (MEGS Specialty Gases, 10 mL_S min^{-1}), and subsequently analyzed by a mass spectrometer (Pfeiffer Omnistar GSD 301) calibrated for CO_2 (m/z

= 44). The gas flow rates were controlled by respective calibrated Vögtlin red-y smart controllers (± 0.3 % accuracy, Switzerland). Besides CO_2, the MS signal for H_2O at m/z =18 was recorded as well.

Temperature programmed oxidation with thermogravimetric analysis (TPO-TGA) was carried out for both fresh and spent GaN and GaN/SBA15 catalysts (TGA550, TA Instrument). 10-25 mg of catalyst was first purged for 30 min with N_2 and then heated at the rate of 5 °C min^{-1} to 120 °C to remove the moisture for another 30 min. Subsequently, the catalyst was heated to 950 °C at 5 °C min^{-1} in the presence of air and held at this temperature for 30 min, while the weight change was recorded.

2.3 Catalytic activity measurements

2.3.1 Methane activation

Methane activation experiments were conducted at 700 °C and 1 bar_{abs} in a fixed bed reactor, as described in[12]. A quartz tube (7 mm ID) with a 15-40 µm frit was inserted into a 0.5″ stainless steel reactor with a counter-current flow configuration.

For the experiments, 500 mg of unsupported (GaN) or 100 mg of supported (GaN/SBA15) catalyst was loaded in the quartz tube and then purged with Ar (25 mL_S min^{-1} at room temperature) for 1 h to remove air and moisture. The temperature was subsequently increased to 700 °C (5 °C min^{-1}) under Ar (25 mL_S min^{-1}). Once the temperature was reached, the flow rate of the Ar was reduced to 1 mL_S min^{-1}, and methane (CH_4, 99.999%, Praxair) was added at a rate of 4 mL_S min^{-1}. The gas flow rates were controlled by calibrated high-precision (± 0.3%) Vögtlin red-y smart controllers (Switzerland). The resulting CH_4-based gas hourly space velocity (GHSV) was 567 h^{-1} for all the catalysts. The reactor outlet and the transfer lines were electrically heated at 200 °C to prevent condensation of the organic components (e.g., C_6H_6, C_7H_8, $C_{10}H_8$). A calibrated quadrupole mass spectrometer (Pfeiffer Omnistar GSD 301) was used for product gas analysis. The instrument was used in multiple ions detection (MID) mode to identify and quantify H_2 (m/z = 2), CH_4 (m/z = 15), C_2H_4 (m/z = 28), C_3H_6 (m/z = 42), CO_2 (m/z = 44), C_6H_6 (m/z = 78), C_7H_8 (m/z = 91), and $C_{10}H_8$ (m/z = 128) with Ar (m/z = 40) as the internal standard. The mass spectrometer was calibrated using calibration cylinders for gases (primary standards with ±1% accuracy) and standard ethanol solutions for benzene (1-1000 ppmV), toluene (1-100 ppmV), and naphthalene (1-10 ppmV). The relative standard deviations (RSD) for calibration factors (from multiple calibration cycles) were less than 1% for the major components (H_2, CH_4, C_2H_4), and less than 5% for the minor components (C_3H_6, C_6H_6, C_7H_8, for $C_{10}H_8$ it was < 10%). The catalyst bed temperature inside the reactor was measured by a K-type thermocouple (Omega Spectris), which controlled the power input to the furnace. The time on stream for GaN and GaN/SBA15 was 7-8 h and 17-18 h, respectively. At the end of the activation experiment, the reactor was purged with Ar at 700 °C for 1 h and then cooled to room temperature under Ar.

CH_4 conversion was calculated based on the gaseous carbon products (eq. 3).

$$x_{CH_4} = \frac{\sum \nu_i \cdot \dot{n}_i}{\dot{n}_{CH_4,in}} \times 100\ [\%] \qquad (3)$$

Where $\dot{n}_i$ denotes the molar flow rate in μmol min^{-1}, while ν_i denotes the number of carbon atoms in the i^{th} species in the product stream (i.e., C_2H_4, C_3H_6, CO_2, C_6H_6, C_7H_8, and $C_{10}H_8$). The denominator represents the molar flow of methane in the feed (μmol min^{-1}). The conversion closely represents the percentage (%) of carbon (C) converted to hydrocarbons and not coke.

2.3.2 Catalyst regeneration

Catalyst regeneration was performed in two different ways; (1) regeneration with air and (2) regeneration with air followed by re-nitridation with NH_3. The unsupported samples were named GaN-R or GaN-RN, while the supported samples were named GaN/SBA15-R or GaN/SBA15-RN. In this notation, -R and -RN stands for regeneration and regeneration-nitridation, corresponding to methods 1 and 2, respectively.

Post-activation, regeneration was carried out in a separate but identical reactor setup as described above to avoid exposing the stainless steel to alternate reducing and oxidizing atmospheres. Preliminary tests showed that when multiple activation regeneration cycles were conducted in the same reactor, the iron oxide of the reactor housing reacted with methane (not shown).

The quartz tube containing the used catalyst, which was distinctly black (Figure S1), was removed from the activation setup and installed in the regeneration setup. Then spent catalyst was first purged with Ar for 1 h (20 mL_S min^{-1}) at room temperature, and then the temperature was increased under Ar to the regeneration temperature (500 °C for GaN, and 550 °C for GaN/SBA15) at a heating rate of 5 °C min^{-1}. The GaN and GaN/SBA15 catalysts were regenerated with air for 4.25 h and 3.25 h, respectively. After the regeneration step, the samples were purged under Ar for 20 h at 700 °C to remove any physisorbed species such as CO_2, O_2, and N_2 from the catalyst and reactor. For method 1, the reactor was then cooled to room temperature under Ar. The quartz tube with the regenerated catalyst was reinstalled in the activation set-up for the second activation cycle, and this process was repeated for each subsequent cycle. A total of five activation and four intermediate regeneration cycles were carried out. Once completed, the spent catalysts (last cycle) were designated as GaN-R or GaN/SBA15-R.

For method 2, after regeneration with air and purging with Ar (for 20 h), the catalysts were re-nitridated with NH_3 (20 mL_S min^{-1}) for 12 h. The unsupported catalysts were re-nitridated at 750 °C, while the supported catalysts were re-nitridated at 700 °C. After cooling down, the catalysts were purged with Ar (20 mL_S min^{-1}) for 1 h to remove any remaining NH_3. The quartz tube was then reinserted into the activation setup. The spent catalyst at the end of 3 activation cycles (with 2 intermediate regenerations/re-nitridations) were designated as GaN-RN or GaN/SBA15-RN.

Alternate regenerating agents such as H_2 and CO_2 were also tested utilizing temperature-programmed experiments. For the former, 100 mg of spent unsupported GaN catalyst was heated from room temperature to 950 °C at 2.5 °C min^{-1} under 40% H_2 (balance 10 mL_S min^{-1} of Ar); while the product gas was qualitatively analyzed for CH_4 (m/z =15), NH_3 (m/z=17), N_2 (m/z = 28) via mass spectrometry. For CO_2 regeneration, the sample was heated to 1000 °C under pure CO_2 (Praxair, 99.999%), while the mass signal corresponding to CO (m/z = 28) was monitored.

Methane activation and regeneration (with air) over GaN/SBA15 catalyst following method 1 was also conducted by means of TGA experiments (Netzsch TA 209 F1 Libra). For that purpose, ~20 mg of catalyst was loaded in the alumina crucible and dried prior to the experiments at 150 °C (under Ar 20 mL_S min^{-1}). Methane activation was carried out at 700 °C for 24 h, followed by a 4.25 h regeneration step with air (20 mL_S min^{-1}, in a 1:1 air-Ar mixture) at 550 °C. In between the activation and regeneration, the sample was flushed for 5 h with Ar (20 mL_S min^{-1}). A single activation cycle (17 h) was also carried out with unsupported GaN (120 mg), without regeneration.

3 Results and Discussion

3.1 Catalyst Characterization

Table 1 summarizes the results of the N_2 adsorption/desorption measurements for the fresh and spent catalyst samples. The unsupported samples had a much smaller total surface area and pore volume than the supported samples (i.e., by a factor of 20). Moreover, they exhibited a bimodal pore size distribution at around 9 and 30 nm, whereas the SBA-15 supported nitride catalyst had a narrow pore size distribution of 7-8 nm (Table 1). Nitrogen adsorption and desorption isotherms, along with the pore size distributions are illustrated in Figure S2.

After the impregnation of the support with gallium, the total surface area decreased by more than 50% from 912 to 426 m^2 g^{-1}. After the nitridation step, the BET surface area was further reduced for both the unsupported and supported samples. The reduction in area was most likely due to a collapse of the pore structure as well as GaN crystallization above the calcination temperature[21].

Table 1. Nitrogen adsorption and desorption results for unsupported and supported fresh and spent catalysts.

Sample	S_{BET}[a] [m^2 g^{-1}]	V_{Pore}[b] [cm^3 g^{-1}]	D_{Pore}[c] [nm]
Ga_2O_3	35	0.13	9.4, 29.3
GaN (fresh)	17	0.06	9.2, 29.6
GaN-RN (3 cycles)	18	0.09	9.2, 29.6
GaN-R (5 cycles)	8	0.11	8.7, 47.8
SBA15	912	0.89	7.9
Ga_2O_3/SBA15	426	0.53	7.9
GaN/SBA15 (fresh)	398	0.49	7.0
GaN/SBA15-RN (3 cycles)	376	0.54	7.0
GaN/SBA15-R (5 cycles)	329	0.49	6.4

[a] S_{BET} = BET total specific surface area obtained from adsorption data in the p/p^0 range from 0.06-0.2; all reported data are within ± 4 m^2 g^{-1} for unsupported and ± 10 m^2 g^{-1} for supported samples based on the repeated analysis.

[b] V_{Pore} = pore volume was obtained at $p/p^0 = 0.9$

[c] D_{Pore} = calculated using the Barrett-Joyner-Halenda (BJH) method;

ICP-OES was used to confirm the presence of gallium in GaN/SBA15. Results showed that the actual Ga loading was 15.0 ± 1.0 wt%, which is very close to the theoretical loading of 16 wt%. The difference of around 1 wt% from the target loading was attributed to the loss of gallium during catalyst synthesis.

Based on the total nitrogen analysis of the unsupported samples, a Ga_2O_3 conversion of 85.6 ± 0.8% was determined. The total nitrogen content, and hence the Ga_2O_3 conversion for the supported samples could not be determined as our method did not allow for Ga dissolution. However, due to the high surface area support and the small gallium-oxide crystallite size of 3-6 nm (observed with TEM), a complete Ga_2O_3 conversion to GaN may be assumed[12].

XRD patterns of the fresh and spent catalysts are illustrated in Figure 1. The reference pattern of β-Ga_2O_3 (2θ = 31.7°, 35.2°, 38.4°, 64.7°; PDF# 04-013-1733) and GaN (2θ = 32.5°, 36.9°, 57.9°; PDF #00-006-0523) were taken from the International Centre for Diffraction Data (ICDD). The unsupported non-nitridated sample exhibited a pattern for β-Ga_2O_3 only, whereas all of the nitridated samples (fresh and used) showed only diffraction patterns corresponding to GaN (Figure 1A). The nitridated gallium-containing supported catalysts showed signs of crystalline GaN but did not exhibit any peaks corresponding to β-Ga_2O_3 (Figure 1B). Even for the Ga_2O_3/SBA15 samples, no diffraction patterns for β-Ga_2O_3 were observed, indicating non-crystalline particles. This was further confirmed with TEM, as reported in our previous work[12]. During the nitridation of the supported samples, the amorphous Ga_2O_3 was converted to crystalline GaN, which exhibited sharp peaks corresponding to this nitride.

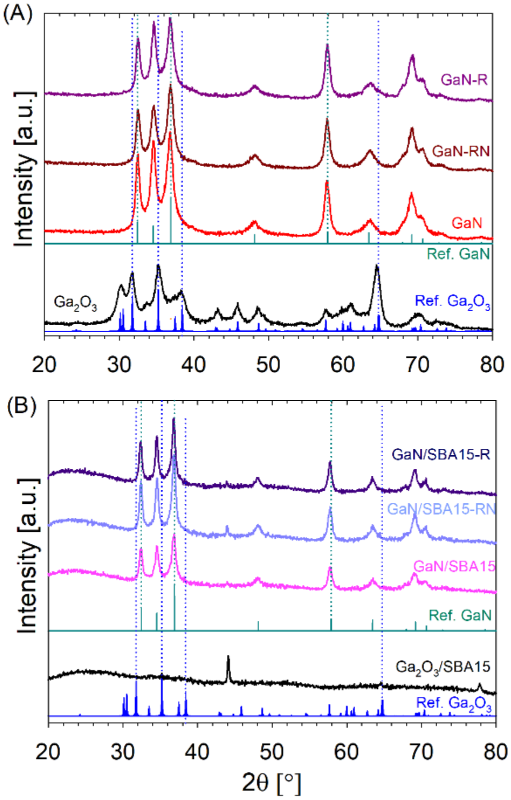

Figure 1. XRD pattern for (A) unsupported and (B) supported catalysts in comparison with references.

SEM-EDS analysis for the fresh GaN catalysts is illustrated in the supporting information Figure S3. Fresh GaN had an almost equimolar Ga (38.2 ± 1.5%) and N (40.7 ± 4.7%) content, with a balance of C (9.7 ± 2.8%) and O (11.3 ± 1.8%).

3.2 Activity measurements

Unsupported and supported GaN catalysts behaved differently during methane activation, as depicted in Figure 2. GaN achieved an initial CH_4 conversion of 3%, which decreased to less than 1% after 1 h on stream and reached a value of ~0.5% after 8 h. During the first hour, the empty catalytic sites (Ga-N) were covered by CH_3* due to the dissociative adsorption of CH_4. Activation experiments conducted in the TGA confirmed this behavior, as depicted in Figure S4. In the first hour, the rate of surface carbon formation reached a maximum and then decreased to a constant value for the remaining 15 h. The unsupported catalyst deactivates faster than the supported one. Supported GaN/SBA15 was able to approach half the rate of the unsupported in 24 h (lower coke formation rate), which indicates its stability. GaN/SBA15 had a rather stable CH_4 conversion of 0.4%. Note, since the unsupported GaN contained more than 20 times more gallium than the supported GaN/SBA15 sample, the values for the CH_4 conversion was similar.

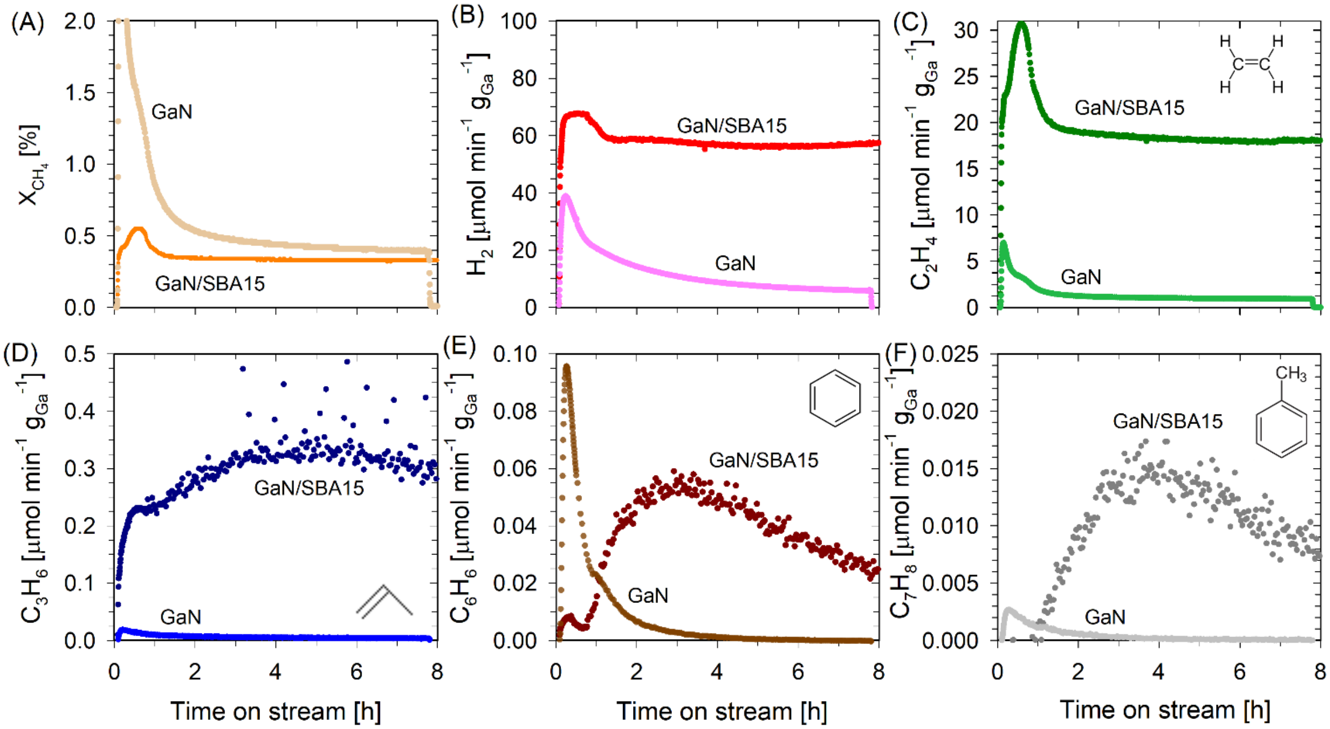

Figure 2. (A) CH_4 conversion, and product formation rates for (B) H_2, (C) C_2H_4, (D) C_3H_6, (E) C_6H_6 and (F) C_7H_{10} as a function of time on stream for unsupported GaN and supported GaN/SBA15 catalyst at T = 700 °C and p = 1.0 bar$_{abs}$.

However, the product formation rates per gram of gallium clearly show that the supported GaN/SBA15 catalyst was more active than the GaN catalyst. The main hydrocarbon product was C_2H_4 with formation rates of ~20 µmol min^{-1} g$_{Ga}^{-1}$ for GaN/SBA15 and less than 2 µmol min^{-1} g$_{Ga}^{-1}$ for GaN (Figure 2C). Propylene, benzene, and toluene were smaller by a factor of more than 100. Notably, GaN produced more benzene and toluene in the first 1 h than the GaN/SBA15. However, after 2 h on stream, the benzene and toluene formation rates were negligible.

3.3 Regeneration cycles

3.3.1 Regeneration medium

Hydrogen, carbon dioxide, and air have been tested as possible regeneration agents. Hydrogen was not suitable as temperatures over 800 °C were needed to remove carbon in the form of CH_4 (Figure S5A). Moreover, under the reducing H_2 atmosphere, GaN decomposed into NH_3 and N_2 above 720 °C and 900 °C, respectively (Figure S5B and C). As a result, gallium metal was produced, which appeared as a shiny metallic coating on the quartz reactor (Figure S5D). A blank experiment conducted with an empty reactor did not produce any CH_4, $NH_{3,}$ and N_2 (not shown).

Carbon dioxide was also not a suitable regeneration agent. Again, temperatures over 800 °C were needed to remove carbon in the form of CO (i.e., $CO_2 + C \rightarrow 2\ CO$), as illustrated in Figure S6. Furthermore, GaN decomposed at temperatures higher than 850 °C (Figure S6A and C). Thermodynamically, GaN decomposition to Ga_2O_3 and N_2 (m/z = 28) is favored in the presence of CO_2 at temperatures higher than 850 °C. Both N_2 and CO (m/z = 28) were produced at 1000 °C, indicated by a higher peak intensity at m/z = 28 (Figure S6C) for the spent GaN sample when compared with the blank run, and the spent Ga_2O_3 (no N). The peak at 900 °C corresponds to the removal of carbon from the GaN surface, which was about 100 °C higher than that of the Ga_2O_3 catalyst. This might indicate a stronger carbon-gallium interaction on the GaN sample.

Air as a regeneration agent was very suitable as the carbon deposition was removed at temperatures between 450 to 500 °C for GaN and between 550 to 600 °C for GaN/SBA15. TPO-TGA (weight change) and TPO-MS (CO_2 and H_2O formation) experiments yielded the same temperatures as depicted in Figure 3. The confinement effect[22] can explain the higher temperature required to regenerate the supported catalyst as the SBA-15 support has an average pore diameter of 7 to 8 nm. At higher temperatures, GaN started to oxidize, which is indicated by a significant weight increase. For pure GaN, an increase of the weight by 12 wt% would be achieved for complete oxidation to Ga_2O_3. Since the unsupported catalyst contained 14.4 wt% Ga_2O_3 and 85.6 wt% GaN, the increase of 9.5 wt% was very close to the theoretical value of 10.2 wt% (Figure 3A). Based on these results, GaN and GaN/SBA15 catalysts were regenerated at 500 °C and 550 °C, respectively.

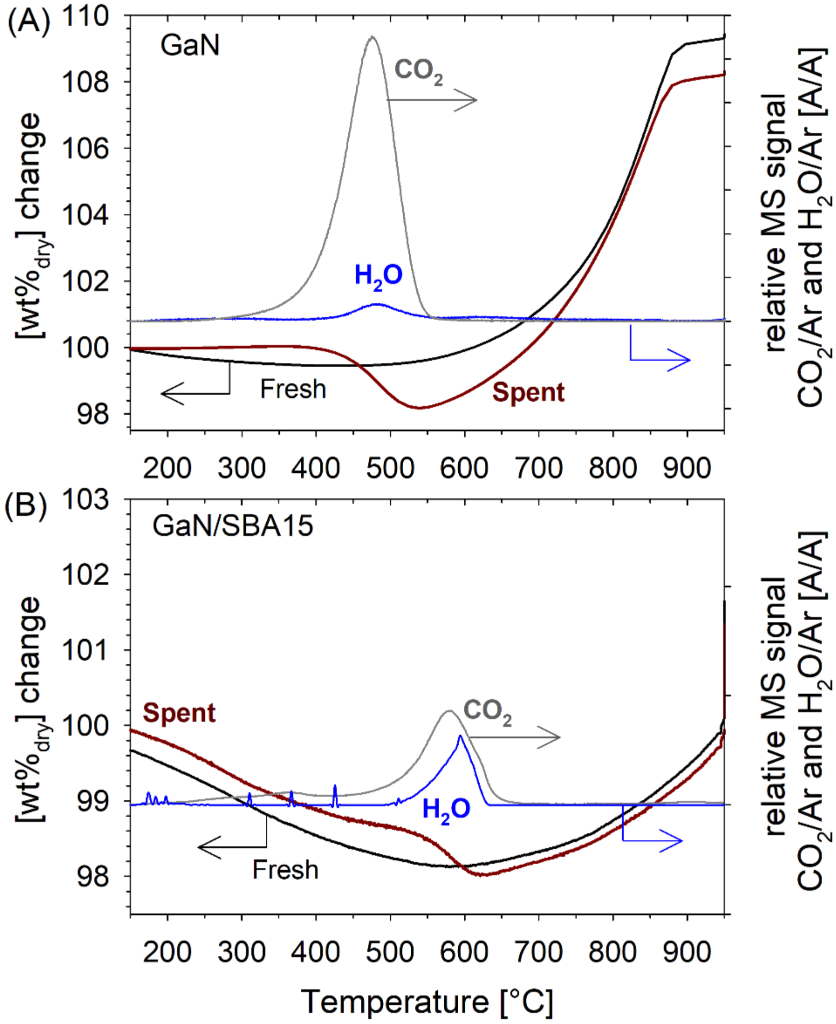

Figure 3. TPO (MS and TGA) results for fresh and used (A) unsupported GaN and (B) supported GaN/SBA15 catalyst.

3.3.2 Reference activation/regeneration cycle

The reference activation/regeneration cycle refers to method 1, in which the catalyst was subjected to 8 h (18 h for GaN/SBA15) activation at 700 °C followed by regeneration in air at 500 °C for 4.25 h (550 °C for 3.25 h for GaN/SBA15) for 5 cycles. For the unsupported GaN catalyst, the results in terms of CH_4 conversion and product formation rate is illustrated in Figure 4.

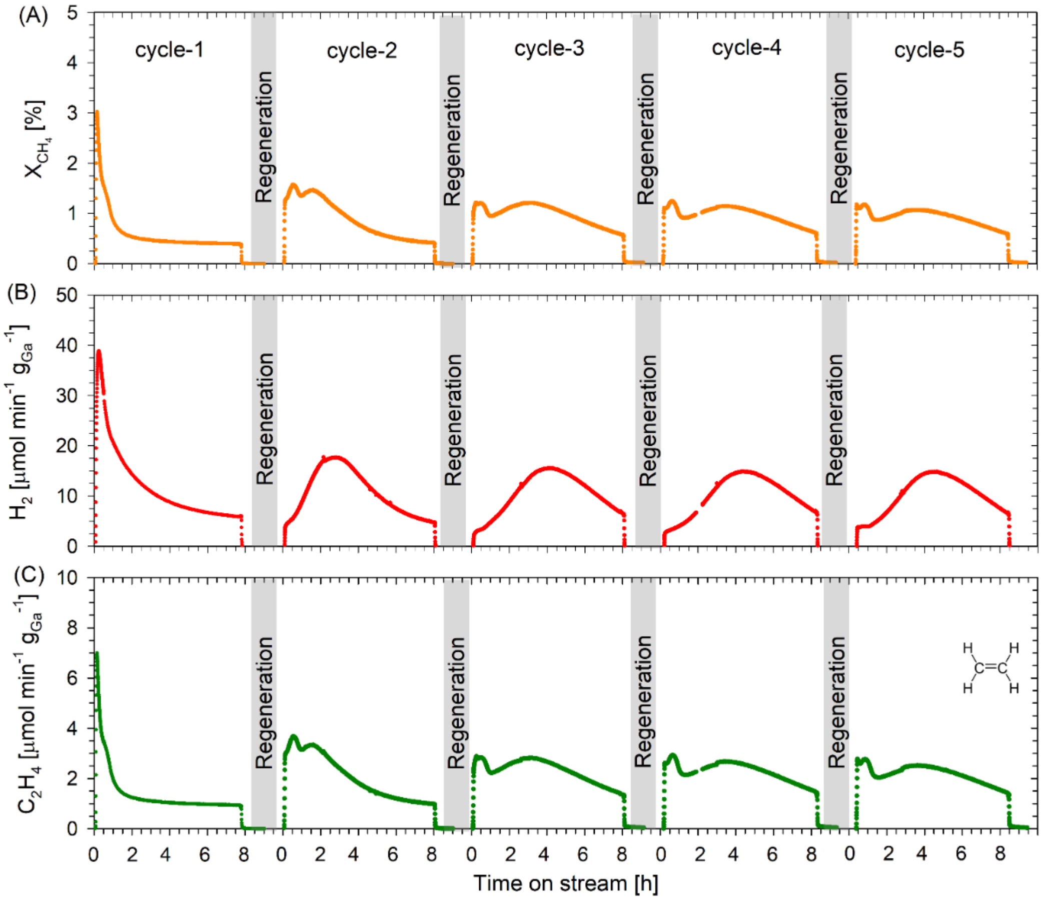

Figure 4. (A) CH_4 conversion and product formation rate of (B) H_2 and (C) C_2H_4 as a function of time on stream over unsupported GaN used in 5 activation cycles with 4 intermediate regeneration steps in air (GaN-R). Activation: 700 °C with 567 h^{-1}, regeneration: air at 500 °C.

The methane activation behavior changed significantly from the 2nd cycle onwards. In detail, the maximum CH_4 conversion, as well as product formation rates, shifted to later times (Figure 4). The reason for this change was the slight surface oxidation of GaN to Ga_2O_3 during the regeneration in air, which had its own unique CH_4 activation behavior, as described in our previous work. During the initial CH_4 adsorption onto Ga_2O_3, the hydrogen in CH_4 reacts with lattice oxygen to form CO_2 (Figure S7A) as well as H_2O and CO (not shown), which has been confirmed via DFT modeling in our previous study[18].

The higher the amount of Ga_2O_3 formed during the regeneration process, the more H_2O and CO_2 (and CO) were produced, resulting in a shift of the H_2 and C_2H_4 formation rates. Note, the nominal mass to charge ratio (m/z) of 28 corresponds to C_2H_4 as well as to CO and N_2. GaN material is stable under reaction conditions and does not decompose (releasing N_2). A significant part of the first peak in Figure 4C for cycles 2 to 5 could be associated with CO formed on surface Ga_2O_3, while the second peak could be attributed to C_2H_4.

In terms of the minor products propylene, benzene, and toluene, their formation rates decreased and shifted with each cycle (Figure S8). Moreover, after 6 h on stream, no benzene, toluene, and naphthalene were produced as the catalyst seemed to deactivate rather fast.

The supported GaN/SBA15 catalysts were more stable (despite a low CH_4 conversion) and active (per gram of gallium) when compared to the unsupported catalysts, as illustrated in Figure 5, and Figure S9. Even after 4 regeneration cycles with air, both the CH_4 conversion and C_2H_4 formation rates were steady throughout each methane activation cycle of 17 h each (X_{CH4} = 0.4; $n_{C_2H_4}$ = 20 µmol min^{-1} g_{Ga}^{-1}). As before, the formation rates of C_3H_6, C_6H_6, and C_7H_8 were over 100 times lower than that of the desired C_2H_4 and were decreasing with each new cycle (Figure S9).

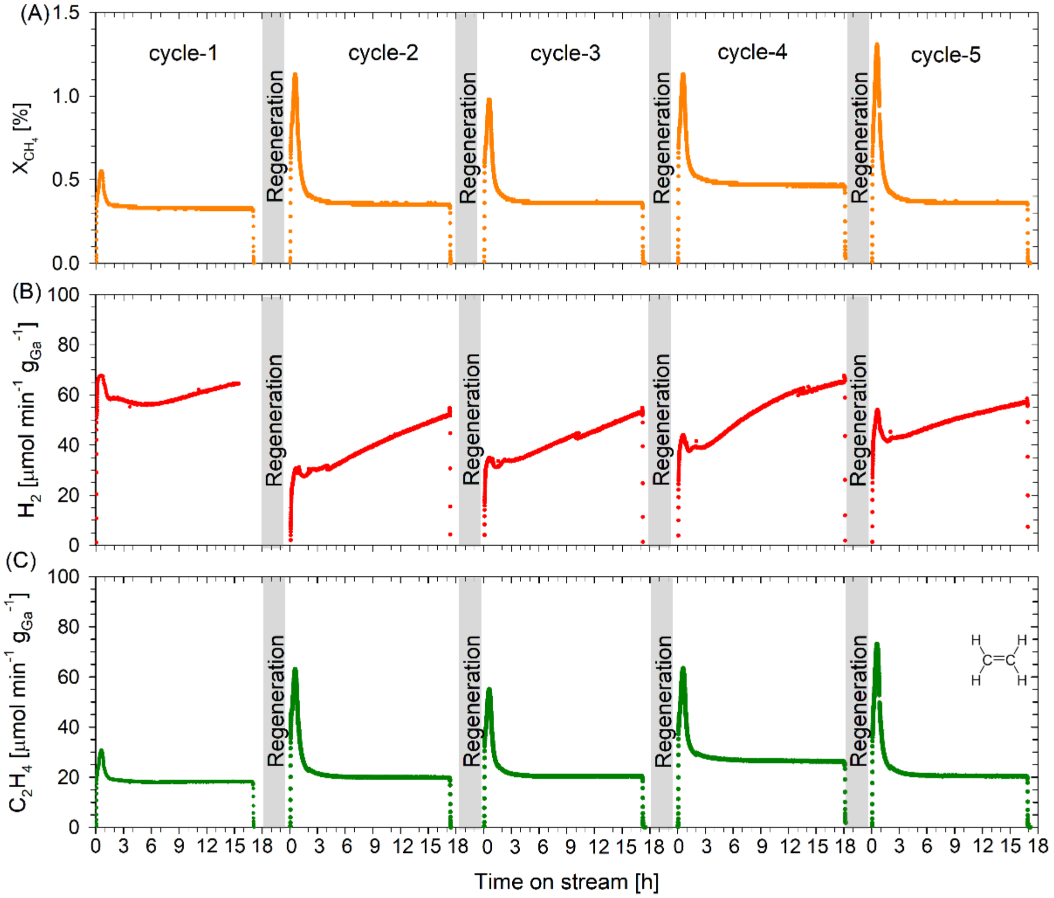

Figure 5. (A) CH_4 conversion and product formation rates for (B) H_2 and (C) C_2H_4 as a function of time on stream over supported GaN/SBA15 used in 5 activation cycles with 4 intermediate regeneration steps in air (GaN/SBA15-R). Activation: 700 °C with 567 h^{-1}, regeneration: air at 550 °C.

The higher CH_4 conversion at the beginning of each activation cycle can be explained by the fact that CH_4 adsorbed on free active sites. It is hypothesized that the dissociative methane adsorption on Ga (i.e., first C–H bond cleavage and formation of CH_3*) is rather fast, while the second C–H bond cleavage and formation of a CH_2* surface complex over a Ga–N hollow site is the rate-determining step[18]. Additionally, at the onset of the 2nd to 5th activation cycle, an elevated CO_2 concentration was measured due to the reaction of the lattice oxygen from Ga_2O_3 with CH_4, as described above (Figure S7B). In the first cycle, no CO_2 was formed as the gallium catalyst was in nitride form.

The product selectivity after each cycle is summarized in Table 2. For both GaN and GaN/SBA15, ethylene selectivities of 97% were achieved in the first cycle, which slightly increased to 99% for the subsequent cycles as the selectivities of the minor product species decreased. In addition, as mentioned before, the amount of produced CO (same nominal mass to charge ratio as C_2H_4) in the 2nd to 5th cycle was unknown but contributed to the increase in the calculated observed C_2H_4 selectivity value as well. Thus, the real C_2H_4 selectivities might actually decrease with each cycle.

Table 2. Product selectivity for GaN and GaN/SBA catalyst (activation/regeneration).

	Catalyst	**Product selectivity* [mol%]**					
		C_2H_4	**C_3H_6**	**C_6H_6**	**C_7H_8**	**$C_{10}H_8$**	**CO_2**
GaN-R	GaN (cycle 1)	97.3	0.65	1.88	0.11	0.02	0.05
	GaN (cycle 2)[#]	97.4	0.32	1.82	0.18	0.04	0.26
	GaN (cycle 3)	98.0	0.24	1.27	0.14	0.03	0.31
	GaN (cycle 4)	98.3	0.21	1.05	0.11	0.02	0.30
	GaN (cycle 5)	98.7	0.17	0.86	0.04	0.00	0.24
GaN/SBA15-R	GaN/SBA15 (cycle 1)	97.4	2.04	0.37	0.12	0.01	0.03
	GaN/SBA15 (cycle 2)[#]	97.9	0.55	0.13	0.04	0.03	1.37
	GaN/SBA15 (cycle 3)	98.3	0.41	0.11	0.03	0.03	1.11
	GaN/SBA15 (cycle 4)	99.0	0.14	0.06	0.02	0.01	0.81
	GaN/SBA15 (cycle 5)	98.3	0.28	0.06	0.02	0.01	1.37

* based on gaseous carbon species (C_2H_4, C_3H_6, C_6H_6, C_7H_8, $C_{10}H_8$, CO_2) without adsorbed carbon species.

[#] from 2nd cycle onwards, actual C_2H_4 selectivity is lower because of the contribution by CO to mass 28.

3.3.3 Optimized activation/regeneration cycle

To decrease the amount of surface Ga_2O_3, a re-nitridation of the regenerated catalyst was carried out. Thus, the subsequent activation cycles displayed similar behavior as the first cycle (Figs. 6 and 7). After the regeneration in air and subsequent re-nitridation with NH_3, the initial CH_4 conversion was ~2.5%. Just like the fresh catalyst (cycle 1), the conversion declined to 0.4% after 7 h, which was reproducible. In addition, the catalyst appeared to be more stable when both regeneration and re-nitridation were performed.

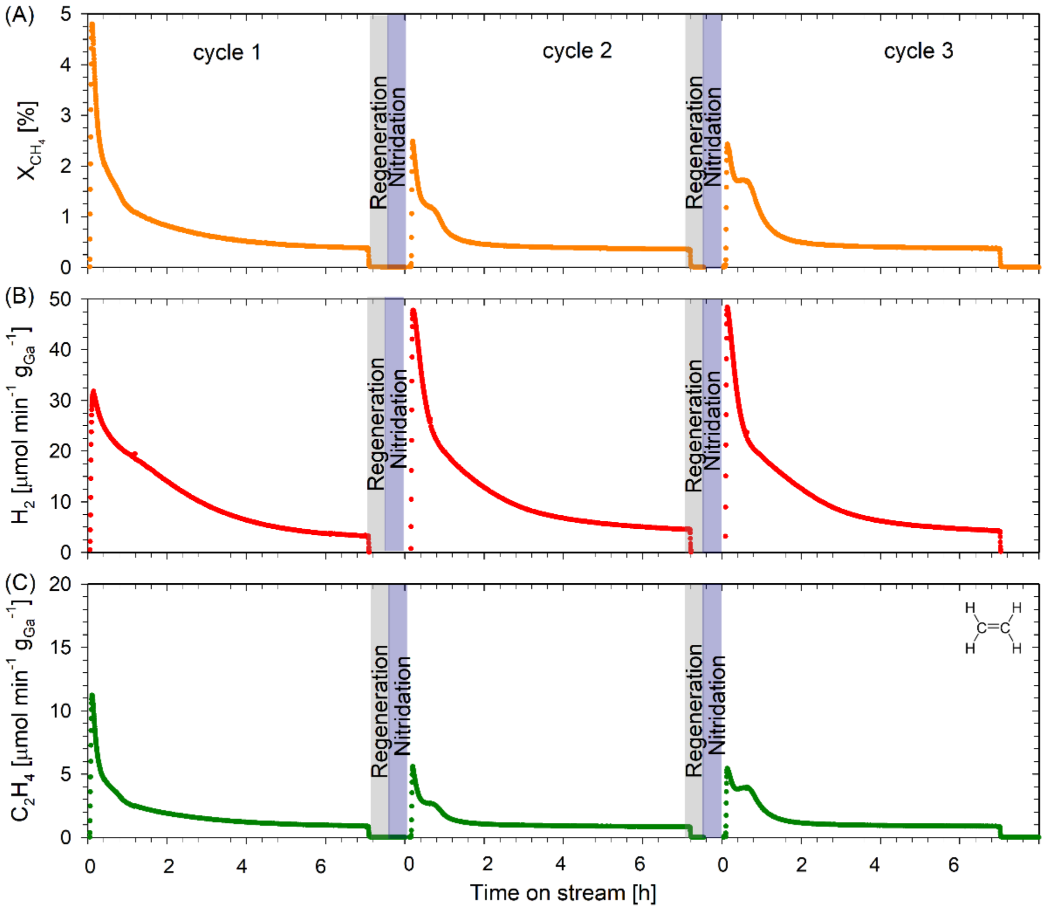

Figure 6. (A) CH_4 conversion and product formation rates for (B) H_2 and (C) C_2H_4 as a function of time on stream over unsupported GaN catalyst with 3 activation cycles and 2 intermediate regeneration and re-nitridation steps (GaN-RN). Activation: 700 °C with 567 h^{-1}, regeneration with air at 500 °C and re-nitridation with NH_3 at 750 °C.

The maximum H_2 rate reached in cycle 1 was 32 μmol min^{-1} g_{Ga}^{-1}. This rate increased by 45% to 48 μmol min^{-1} g_{Ga}^{-1} during cycle 2 and remained steady throughout cycle 3. After 7 h on stream, the H_2 production rate decreased steadily to 4 μmol min^{-1} g_{Ga}^{-1}. The C_2H_4 formation in the second and third cycles reached steady state at a rate of about 1 μmol min^{-1} g_{Ga}^{-1}, corresponding to a CH_4 conversion of 0.4%. Aromatic compounds such as benzene and toluene were only produced at the beginning of each cycle when the active GaN surface was free. Once CH_4 conversion and C_2H_4 formation reached a steady-state, the aromatic species molar rates became zero (Figure S10).

Again, the supported GaN/SBA15 catalyst was more active and stable compared to the unsupported GaN catalyst (Figure 7). After regeneration in air and subsequent re-nitridation in NH_3, the active surface sites (Ga-N) were empty, enabling a high CH_4 conversion in the first hour of each activation cycle. Ethylene formation rates were about the same for each cycle with a steady-state value of 20 µmol min^{-1} g_{Ga}^{-1}. However, the H_2 formation rates in the 2nd and 3rd cycles were lower than in the first cycle but constant with time on stream. In addition, the formation of minor species (C_3H_6, C_6H_6, and C_7H_8) decreased slightly with each cycle (Figure S11).

CO_2 formation for the re-nitridated catalysts (GaN-RN and GaN/SBA15-RN) was much smaller when compared to that of the catalyst that was only regenerated (GaN-R and GaN/SBA15-R) as depicted in Figure S7.

The main difference between the two regeneration methods was the H_2 and CO_2 formation rates. The samples that underwent re-nitridation formed H_2O (not shown) and CO_2 (Figure S7) at the beginning of each cycle, resulting in a slower H_2 formation rate at the start. The same trend was also shown for supported Ga_2O_3/SBA-15 catalysts in our previous work[12].

The product selectivities did not change significantly with each cycle. The selectivity of 97 to 98% was achieved for C_2H_4 with both types of catalysts (Table 3). The unsupported catalyst exhibited a slightly higher C_6H_6 selectivity than the supported sample, whereas the opposite was observed for C_3H_6.

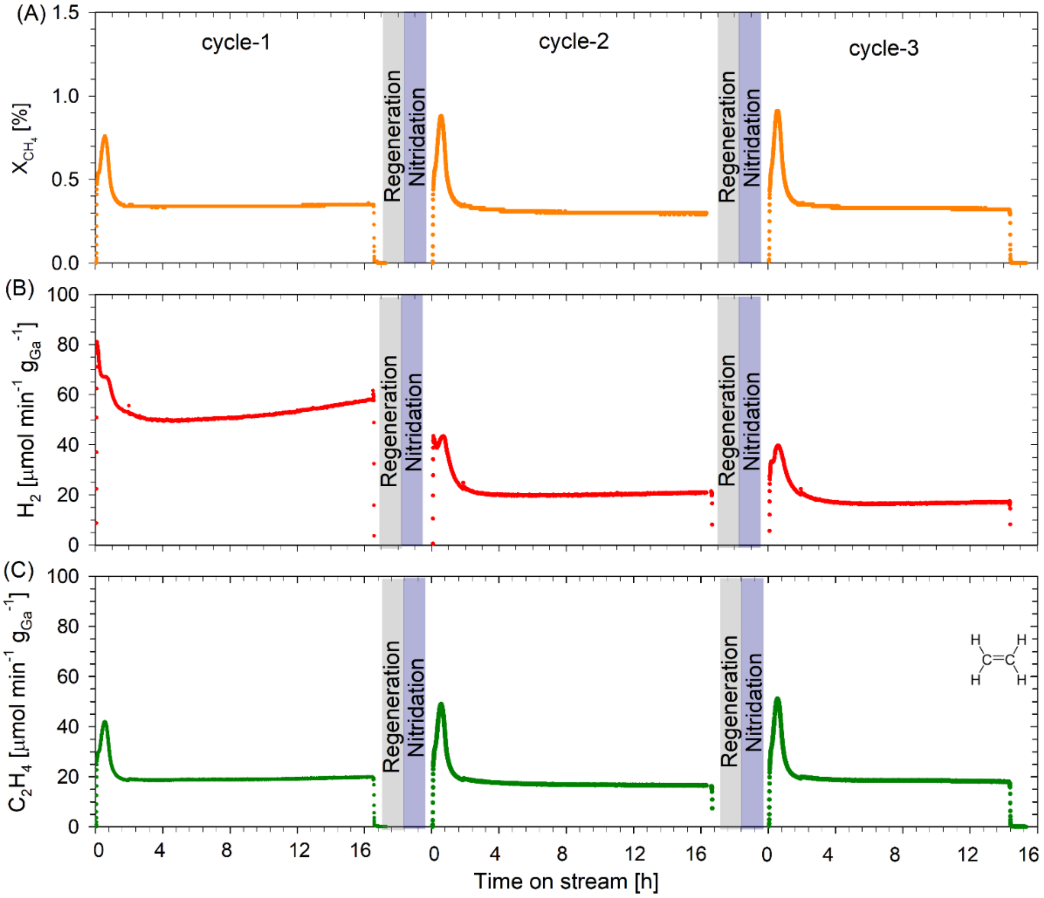

Figure 7. CH_4 conversion and product formation rates for (B) H_2 and (C) C_2H_4 as a function of time on stream over supported GaN catalysts with 3 activation cycles and 2 intermediate regenerations and re-nitridation steps (GaN/SBA15-RN). Activation: 700 °C with 567 h^{-1}, regeneration with air at 550 °C and re-nitridation with NH_3 at 700 °C.

Table 3. Product selectivity for GaN-RN and GaN/SBA15-RN catalysts (activation/regeneration/re-nitridation).

	Catalyst	**Gas selectivity [mol%]**					
		C_2H_4	**C_3H_6**	**C_6H_6**	**C_7H_8**	**$C_{10}H_8$**	**CO_2**
GaN-RN	GaN (cycle 1)	97.7	0.43	1.57	0.13	0.03	–
	GaN (cycle 2)	97.1	1.01	1.68	0.09	0.03	–
	GaN (cycle 3)	97.5	0.85	1.32	0.07	0.02	–
GaN/ SBA15-RN	GaN/SBA15 (cycle 1)	98.0	1.49	0.21	0.06	0.01	–
	GaN/SBA15 (cycle 2)	97.7	1.52	0.15	0.10	0.01	–
	GaN/SBA15 (cycle 3)	98.2	0.98	0.07	0.05	0.00	–

3.3.4 Characterization of used catalyst

Temperature programmed oxidation - mass spectrometry (TPO-MS) was performed on the fresh and spent catalysts to estimate the amount of adsorbed carbon produced during the methane activation. For both the supported and unsupported catalysts, only the spent catalysts after the final (3rd or 5th) activation cycle was used. TPO-MS of all the spent unsupported catalysts (GaN-R and GaN-RN) exhibited a single CO_2 peak around 500 °C, as illustrated in Figure S12A, which was very similar to the results presented in Figure 3A. The results indicate that the adsorbed carbon was most likely in amorphous rather than graphitic form. However, the precise type and stoichiometry of the adsorbed carbon (C_xH_y*) is unknown.

Quantitative analyses of the spent catalysts yielded a relative carbon amount of 14 $mg_C\ g_{cat}^{-1}$ for the GaN-R and 19 $mg_C\ g_{cat}^{-1}$ for the GaN-RN catalyst. Approximately 1.1 % of the total CH_4 fed over the span of 8 h was converted to surface carbon in the last activation cycle for the GaN-RN catalyst, while 0.7% was converted to surface carbon in the last activation cycle for the GaN-R catalyst.

The supported catalysts exhibited a single CO_2 peak around 600 °C (Figure S12B), which is 100 °C above the peak displayed by the unsupported ones with 18 and 14 $mg_C\ g_{cat}^{-1}$ for the GaN/SBA15-R and GaN/SBA15-RN (Table S1), respectively. Both supported and unsupported catalysts adsorbed around 15-

20 mg_C g_{cat}^{-1}, which was much smaller than the 43-120 mg_C g_{cat}^{-1} reported over PtSn-zeolite[13]. Considering only the Ga sites, the supported catalysts had around 5 times more surface carbon than the unsupported catalysts (i.e., in mg carbon per gram of Ga). This indicates a better dispersion of the active Ga-N centers. This adsorbed surface carbon is a necessary carbon intermediate (i.e., CH_2* or CH_3*) for the formation of C_2H_4; it also contributes to catalyst deactivation.

Based on the results of the TPO analysis, the overall product selectivities and CH_4 conversions were determined (Table 4). The supported samples were superior due to their higher C_2H_4 selectivity and their tendency to adsorb less carbon. In was also noted that a mild re-nitridation helped suppress GaN oxidation limiting CO_2 and H_2O formation. The unsupported catalyst had a higher CH_4 conversion; however, it also contained 20 times more gallium. Therefore, the supported catalyst was much more active and selective on a per gram gallium.

Table 4. Overall product selectivity and methane conversion for all catalysts.

Catalyst	**Overall selectivity [mol%]**							**X_{CH4} [%]^a**
	C_2H_4	**C_3H_6**	**C_6H_6**	**C_7H_8**	**$C_{10}H_8$**	**CO_2**	**C_{ads}**	**CH_4**
GaN-R	54.7*	0.09	0.47	0.02	0.00	0.13	44.6	1.64
GaN-RN	34.8	0.30	0.47	0.02	0.01	-	64.4	1.70
GaN/SBA15-R	81.2*	0.24	0.05	0.01	0.01	1.13	17.4	0.51
GaN/SBA15-RN	81.3	0.81	0.06	0.04	0.00	-	17.2	0.44

*C_2H_4 selectivity could be lower (by up to 15% points) due to contribution by CO to m/z = 28.

For the spent catalyst GaN-RN, the total surface area remained practically unchanged within the accuracy of the instrument (± 4 m^2 g^{-1}); however, it dropped to 8 m^2 g^{-1} for the GaN-R catalyst (Table 1). For the latter, the decrease in the area might be caused by the continued oxidation of GaN to Ga_2O_3 [11]. The total surface area of the spent supported catalyst GaN/SBA15-RN decreased slightly from 398 to 376 m^2 g^{-1}.

The decrease in surface area for the GaN/SBA15-R catalyst was more significant (398 to 329 m^2 g^{-1}) at 12% (Table 1).

The sample regenerated with air (GaN-R) did not show any diffraction pattern for Ga_2O_3, indicating that the GaN in the bulk phase was not oxidized during the regeneration at 500 °C. However, slight surface oxidation forming amorphous Ga_2O_3 is plausible and also explains the formation of CO_2 and H_2O in the subsequent activation cycle. The used, regenerated (GaN/SBA15-R) and regenerated/re-nitridated (GaN/SBA15-RN) catalysts only showed a GaN diffraction pattern. The XRD peak around $2\theta = 44°$ (Figure 1B) corresponds to the XRD aluminum sample holder.

The spent GaN catalyst also exhibited an equimolar Ga and N content, but with a larger C content (20.1 ± 3.8%) due to adsorbed carbon (Figure S13). The compositions for the GaN-R (Figure S14), GaN-RN (Figure S15), and fresh GaN samples were indistinguishable from one another, which proves that the oxidation in air (at 500 °C) was only superficial and not significant. On the other hand, the spent catalyst treated with 40% H_2 lost 50-80 atomic% N (Figure S16), which was also visible from the evolution of NH_3 and N_2 (Figure S5).

The regenerated and re-nitridated supported catalysts (GaN/SBA15-RN) produced less adsorbed carbon per gram of the catalyst (Table S1) and had a constant C_2H_4 yield. In supported catalysts, GaN is dispersed as 3-5 nm nanoparticles inside SBA-15 pores. Unsupported catalysts (>80% GaN) have lower porosity (Table 1) and a poor dispersion of GaN (only the surface GaN are catalytic while the bulk remained inaccessible to CH_4). The dispersion of the active sites in GaN/SBA15 resulted in lower coke and higher C_2H_4 yields. A similar observation was made for isolated well-dispersed active Fe sites inside SiO_2 for CH_4 conversion to C_2H_4 [9].

Figure S17 visualized the increase of adsorbed carbon as a function of time on stream during the methane activation at 700 °C. In the first cycle, the rate of carbon deposition increased from 2 to 4.5 µmol min^{-1} g_{Cat}^{-1} within 24 h. In the second and third cycles, the rate increased faster and achieved a value of 6 µmol min^{-1} g_{Cat}^{-1} after 24 h. After 24 h on stream, a total carbon deposition of 60 mg g_{Cat}^{-1} for the 1st cycle and 80 mg g_{Cat}^{-1} for the 2nd and 3rd cycles were determined. This was by a factor of 3-4 larger compared to the carbon deposition reported from the packed-bed reactor experiments above with 18 mg g_{Cat}^{-1} for the last run (GaN/SBA15-R). This was expected because TGA experiments were diffusion-limited due to the absence of a convective flow that constantly removes the products from the catalyst bed. After the last activation cycle, the regeneration in air at 550 °C was conducted for more than 12 h, even though 4.25 h were sufficient to remove all carbon surface species. In that extra 8 h, a slight increase in the sample weight of 0.02 mg was detected (<0.13% of the initial mass), indicated a very small surface gallium nitride oxidation.

3.3.5 Reaction mechanism

Based on the experimental results and the published Density Functional Theory (DFT) study[18], the following scheme for the CH_4 activation to C_2H_4 , regeneration in air, and subsequent re-nitridation with NH_3 is presented (Figure 8). CH_4 undergoes fast dissociative chemisorption on GaN with CH_3* adsorbing on Ga^{3+} and H* on the neighboring N^{3-} (see steps R1 and R2 in Figure 8). The rate-determining step is the cleavage of CH_3* into CH_2* and H* on Ga (step R4), whereas the coupling of two CH_2* species to C_2H_4 (step R5) is rather fast. The surface intermediate CH_2* can also form C_3H_6 and C_6H_6 (not shown), and even less reactive carbon surface species such as CH*, C* and C_xH_y* (step R6). The latter, with a yet unknown stoichiometry, could include polynuclear aromatic compounds. During the regeneration in air at 450-550 °C, the carbon surface species are combusted to CO_2 and H_2O (step R7). However, at the same time, part of the surface GaN is oxidized to Ga_2O_3. A re-nitridation with NH_3 converts the surface Ga_2O_3 layer back to GaN (step R8) to keep the initial activity.

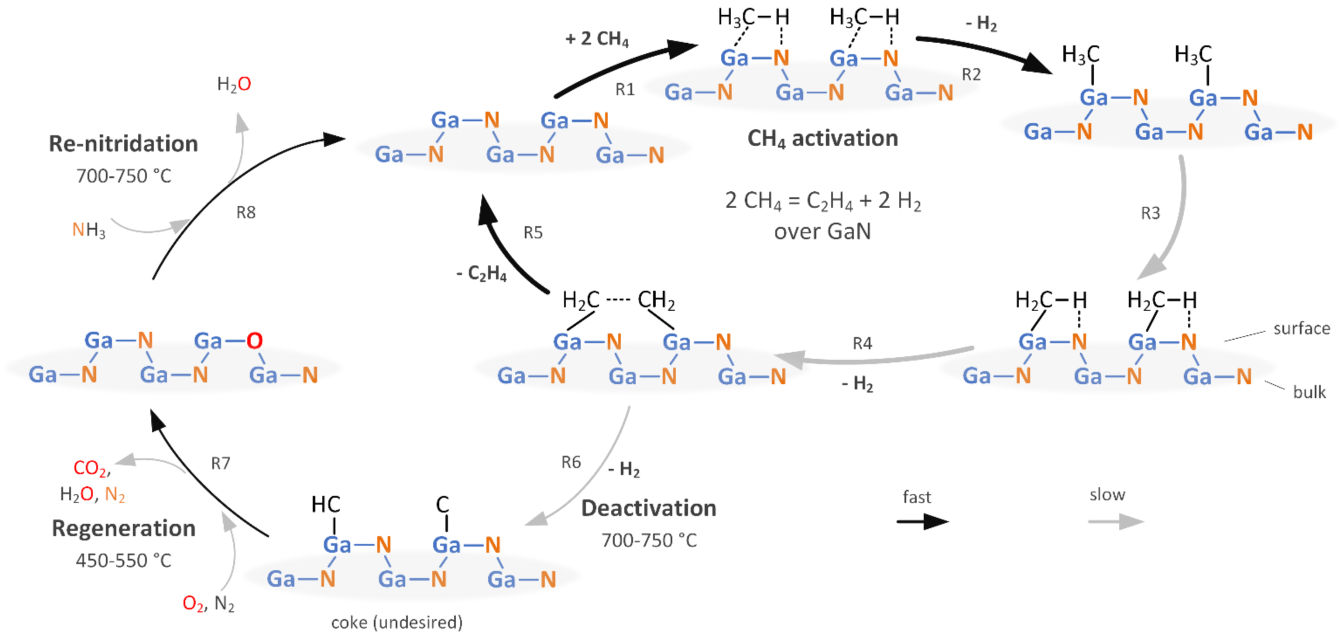

Figure 8. Proposed mechanism for the optimized activation/regeneration/re-nitridation cycle.

3.4 Long term test

The supported catalysts displayed greater stability and larger hydrogen and ethylene yields per gram of gallium. Therefore, a long-term run (150 h) was completed using the GaN/SBA15 catalyst. The activation temperature was initially maintained at 700 °C for 100 h, then increased (at 5 °C min^{-1}) to and held constant at 750 °C for 24 h, before finally being decreased (at 5 °C min^{-1}) to and maintained at 700 °C for another 24 h. The yields of the major (H_2 and C_2H_4, Figure 9) and minor products (C_3H_6, C_6H_6, and C_7H_{10}, 3-4 orders of magnitude lower than C_2H_4, Figure S18) were nearly stable with a small increase observed for H_2 at 100 h and 700 °C. This change in H_2 yield was probably because of the increased carbon deposition. The production rate of H_2 was steady around 75 μmol min^{-1} g_{Ga}^{-1}, while that of C_2H_4 was constant at 15-16 μmol min^{-1} g_{Ga}^{-1} with C_2H_4 selectivity of 98% (based on gas phase species).

When the temperature was raised to 750 °C, all of the product yields initially increased, but rapidly declined after that. They continued decreasing as the temperature was lowered to 700 °C (after 24 h at 750 °C) and the catalyst lost nearly all its activity. Around half of all the H_2 formed was produced in the first 100 h at 700 °C. Another 40% of the total H_2 yield was achieved in the subsequent 24 h at 750 °C. This represents around a 250% increase in H_2 production at 750 °C, an indication of rapid carbon deposition. This was further supported by a modest 24% increase of C_2H_4 output. The loss of stability and decrease in yield, which occurred within the first 30 min at 750 °C, also supports rapid catalyst coking (see step R6 in Fig 8.). TPO-MS of the spent catalyst exhibited the CO_2, and H_2O peaks, both at approximately 600 °C (Figure S19). A total carbon deposition of 237 $mg_C\ g_{Cat}^{-1}$ was determined, which was around 10 times greater than for the catalysts discussed in the previous sections (Table S1). Temperatures of lower than 750 °C are recommended for the non-oxidative methane dehydrogenation and subsequent coupling to ethylene.

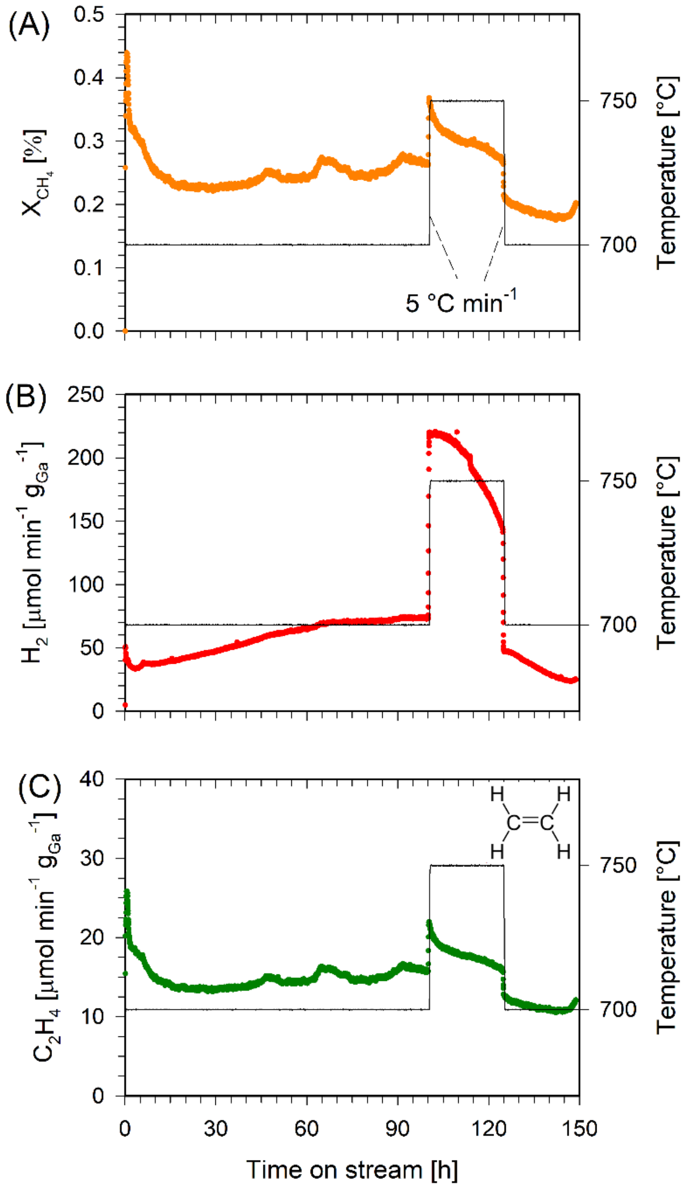

Figure 9. (A) CH_4 conversion and product formation rates for (B) H_2 and (C) C_2H_4 as a function of time on stream for supported GaN/SBA15 for long term run (150 h).

4 Conclusions

Both supported (GaN/SBA15) and unsupported (GaN) catalysts were synthesized for methane activation studies. The supported GaN/SBA15 catalysts had a 20-40 times higher activity towards C_2H_4 per gram of gallium than the unsupported catalysts. For the unsupported catalyst, a slight reduction in methane activation was observed. All the supported catalysts exhibited excellent and reproducible stability (for

>100 h). Even though the CH_4 conversion was low ($X = 0.4$-0.5), no significant deactivation was observed for the supported samples.

In terms of catalyst regeneration, air was the best regeneration agent as it only required temperatures of 450 to 550 °C to remove the carbon deposition without oxidizing the bulk of the gallium nitride catalyst. Regeneration with H_2 or CO_2, on the other hand, required temperatures of higher than 850 °C at which GaN started to decompose.

GaN and GaN/SBA15 catalysts were used in multiple activation/regeneration and activation/regeneration/re-nitridation cycles. Without a re-nitridation step after regeneration with air, surface Ga_2O_3 was formed, which led to the formation of CO_2, CO, and H_2O at the beginning of each activation cycle. A re-nitridation after the catalyst regeneration is highly recommended as the surface Ga_2O_3 is converted to GaN, which keeps the ethylene yield constant over multiple cycles.

Supporting information

Figures associated with catalyst characterizations (appearance of fresh and spent catalysts, N_2 adsorption isotherms, pore size distribution, SEM-EDS); molar flow rates for the minor components (C_3H_6, C_6H_6, C_7H_8, CO_2, H_2O) as a function of time produced during methane activation runs (including long term run); the products produced during catalyst regeneration with H_2 (CH_4, NH_3, N_2, metallic Ga) and CO_2 (CO and N_2); evolution of CO_2 and H_2O during catalyst regeneration with air; a table for the amount of carbon deposited (mg per g of catalyst) during CH_4 activation runs.

Acknowledgments

The authors thank Aleksandra Djuric for conducting the N_2 adsorption/desorption tests. They also wish to thank Ranjan Roy and Andrew Golsztajn for the ICP-OES measurements and for helping the authors with developing the total nitrogen analysis method. The authors also thank Alexandra Jacobson for her help with proofreading. They acknowledge the financial support from Fonds de recherche du Québec - Nature et technologies Team Grant (FRQNT, PR-253397) and from the Centre in Green Chemistry and Catalysis (FRQNT-2020-RS4-265155-CCVC) as well as from Imperial Oil University Research Award and Natural Sciences and Engineering Research Council of Canada (NSERC CRDPJ 534026).

References

(1) Spath, P. L.; Dayton, D. C. *Preliminary Screening - Technical and Economic Assessment of Synthesis Gas to Fuels and Chemicals with Emphasis on the Potential for Biomass-Derived Syngas*; Technical Report, National Renewable Energy Laboratory: Golden, CO, USA, 2003.

(2) Venkataraman, V. K.; Guthrie, H. D.; Avellanet, R. A.; Driscoll, D. J. Overview of U.S. DOE's Natural Gas-to-Liquids RD&D Program and Commercialization Strategy. In *Studies in Surface Science and Catalysis*; Elsevier, **1998**; Vol. 119, 913–918.

(3) Ma, S.; Guo, X.; Zhao, L.; Scott, S.; Bao, X. Recent Progress in Methane Dehydroaromatization: From Laboratory Curiosities to Promising Technology. *J. Energy Chem.* **2013**, *22* (1), 1–20.

(4) Spivey, J. J.; Hutchings, G. Catalytic Aromatization of Methane. *Chem. Soc. Rev.* **2014**, *43* (3), 792–803.

(5) Karakaya, C.; Kee, R. J. Progress in the Direct Catalytic Conversion of Methane to Fuels and Chemicals. *Prog. Energy Combust. Sci.* **2016**, *55*, 60–97.

(6) Fricke, R.; Kosslick, H.; Lischke, G.; Richter, M. Incorporation of Gallium into Zeolites: Syntheses, Properties and Catalytic Application. *Chem. Rev.* **2000**, *100* (6), 2303–2405.

(7) Liu, B.; Yang, Y.; Sayari, A. Non-Oxidative Dehydroaromatization of Methane over Ga-Promoted Mo/HZSM-5-Based Catalysts. *Appl. Catal. A Gen.* **2001**, *214* (1), 95–102.

(8) Choudhary, V. R.; Kinage, A. K.; Choudhary, T. V. Low-Temperature Nonoxidative Activation of Methane over H-Galloaluminosilicate (MFI) Zeolite. *Science.* **1997**, *275* (5304), 1286–1288.

(9) Guo, X.; Fang, G.; Li, G.; Ma, H.; Fan, H.; Yu, L.; Ma, C.; Wu, X.; Deng, D.; Wei, M.; et al. Direct, Nonoxidative Conversion of Methane to Ethylene, Aromatics, and Hydrogen. *Science.* **2014**, *344* (6184), 616–619.

(10) Li, L.; Fan, S.; Mu, X.; Mi, Z.; Li, C.-J. Photoinduced Conversion of Methane into Benzene over GaN Nanowires. *J. Am. Chem. Soc.* **2014**, *136* (22), 7793–7796.

(11) Li, L.; Mu, X.; Liu, W.; Kong, X.; Fan, S.; Mi, Z.; Li, C. J. Thermal Non-Oxidative Aromatization of Light Alkanes Catalyzed by Gallium Nitride. *Angew. Chemie - Int. Ed.* **2014**, *53* (51), 14106–14109.

(12) Dutta, K.; Chaudhari, V.; Li, C.-J.; Kopyscinski, J. Methane conversion to ethylene over GaN catalysts. Effect of catalyst nitridation. *Appl. Catal. A, Gen.* **2019**, under review.

(13) Gerceker, D.; Motagamwala, A. H.; Rivera-Dones, K. R.; Miller, J. B.; Huber, G. W.; Mavrikakis, M.; Dumesic, J. A. Methane Conversion to Ethylene and Aromatics on PtSn Catalysts. *ACS Catal.* **2017**, *7* (3), 2088–2100.

(14) Pham, H. N.; Sattler, J. J. H. B.; Weckhuysen, B. M.; Datye, A. K. Role of Sn in the Regeneration of Pt/γ-Al2O3 Light Alkane Dehydrogenation Catalysts. *ACS Catal.* **2016**, *6* (4), 2257–2264.

(15) Sun, K.; Ginosar, D. M.; He, T.; Zhang, Y.; Fan, M.; Chen, R. Progress in Nonoxidative Dehydroaromatization of Methane in the Last 6 Years. *Ind. Eng. Chem. Res.* **2018**, *57* (6), 1768–1789.

(16) Kosinov, N.; Coumans, F. J. A. G.; Li, G.; Uslamin, E.; Mezari, B.; Wijpkema, A. S. G.; Pidko, E. A.; Hensen, E. J. M. Stable Mo/HZSM-5 Methane Dehydroaromatization Catalysts Optimized for High-Temperature Calcination-Regeneration. *J. Catal.* **2017**, *346*, 125–133.

(17) Lu, Y.; Xu, Z.; Tian, Z.; Zhang, T.; Lin, L. Methane Aromatization in the Absence of an Added Oxidant and the Bench Scale Reaction Test; *Cat. Letters*. **1999,** *62*, 215-220.

(18) Chaudhari, V.; Dutta, K.; Li, C.-J.; Kopyscinski, J. Mechanistic Insights of Methane Conversion to Ethylene over Gallium Oxide and Gallium Nitride Using Density Functional Theory. *Mol.*

Catal. **2019**, *In-print*. 110606

(19) Aljishi, A.; Veilleux, G.; Hernandez Lalinde, J. A.; Kopyscinski, J. The Effect of Synthesis Parameters on Ordered Mesoporous Nickel Alumina Catalyst for CO_2 Methanation. *Appl. Catal. A Gen.* **2018**, *549*, 263–272.

(20) Zhao, D.; Feng, J.; Huo, Q.; Melosh, N.; Fredrickson, G. H.; Chmelka, B. F.; Stucky, G. D. Triblock Copolymer Syntheses of Mesoporous Silica with Periodic 50 to 300 Angstrom Pores. *Science.* **1998**, *279* (5350), 548–552.

(21) Talapaneni, S. N.; Park, D.; Choy, J.; Ramadass, K.; Elzatahry, A.; Balawi, A. S. Al; Al-Enizi, A. M.; Mori, T.; Vinu, A. Facile Synthesis of Crystalline Nanoporous GaN Templated by Nitrogen Enriched Mesoporous Carbon Nitride for Friedel-Crafts Reaction. *Chem. Sel.* **2016**, *1*, 6062–6068.

(22) Kosinov, N.; Wijpkema, A. S. G.; Uslamin, E.; Rohling, R.; Coumans, F. J. A. G.; Mezari, B.; Parastaev, A.; Poryvaev, A. S.; Fedin, M. V.; Pidko, E. A.; et al. Confined Carbon Mediating Dehydroaromatization of Methane over Mo/ZSM-5. *Angew. Chemie Int. Ed.* **2018**, *57* (4), 1016–1020.